The EMBO Journal Vol.17 No.8 pp.2353–2358, 1998

Structure of wild-type yeast RNA polymerase II and location of Rpb4 and Rpb7

Grant J.Jensen, Gavin Meredith, David A.Bushnell and Roger D.Kornberg[1]

Department of Structural Biology, Stanford University School of Medicine, Stanford, CA 94305, USA

[1]Corresponding author

The three-dimensional structure of wild-type yeast RNA polymerase II has been determined at a nominal resolution of 24 Å. A difference map between this structure and that of the polymerase lacking subunits Rpb4 and Rpb7 showed these two subunits forming part of the floor of the DNA-binding (active center) cleft, and revealed a slight inward movement of the protein domain surrounding the cleft. Surface plasmon resonance measurements showed that Rpb4 and Rpb7 stabilize a minimal pre-initiation complex containing promoter DNA, TATA box-binding protein (TBP), transcription factor TFIIB and the polymerase. These findings suggest that Rpb4 and Rpb7 play a role in coupling the entry of DNA into the active center cleft to closure of the cleft. Such a role can explain why these subunits are necessary for promoter-specific transcription *in vitro* and for a normal stress response *in vivo*.

Keywords: electron crystallography/Rpb4/Rpb7/transcription

Introduction

Nucleic acid polymerase structure has been studied by both X-ray and electron crystallography. To date, only the smaller, single subunit polymerases have been subjected to X-ray analysis, including the bacteriophage T7 RNA polymerase, which is the only RNA polymerase whose structure is known to atomic resolution (Sousa *et al.*, 1993). Lower resolution structures of several multisubunit polymerases have been determined by electron crystallography, including core and holo- *Escherichia coli* RNA polymerase (Darst *et al.*, 1989; Polyakov *et al.*, 1995), yeast RNA polymerase I (Schultz *et al.*, 1990) and a mutant form of yeast RNA polymerase II (Darst *et al.*, 1991a). All polymerase structures obtained by both X-ray and electron crystallography show a large cleft appropriate in size for binding duplex DNA, and further appear to contain a mobile arm allowing open and closed conformations of the cleft, presumably permitting entry and retention of DNA. In the specific case of RNA polymerase II from the yeast *Saccharomyces cerevisiae*, which is the subject of this work, it has been shown that nucleic acid does in fact occupy this cleft in a paused elongation complex (C.L.Poglitsch, G.Meredith, A.Gnatt, G.J.Jensen, W.-h. Chang and R.D.Kornberg, in preparation), and that the arm domain enclosing the cleft is mobile (Asturias *et al.*, 1997).

RNA polymerase II, which catalyzes the transcription of all protein-encoding genes, is composed in yeast of 12 unique subunits denoted Rpb1–Rpb12. Two of these subunits, Rpb4 and Rpb7, form a dissociable subcomplex (Dezelee *et al.*, 1976; Ruet *et al.*, 1980; Edwards *et al.*, 1991), present in substoichiometric amounts during exponential growth (Choder and Young, 1993). This complex has been implicated in the stress response and in the initiation of transcription (Woychik and Young, 1989; Edwards *et al.*, 1991; Choder and Young, 1993). Human homologs of Rpb4 and Rpb7 have been identified and have also been shown to form a dissociable subcomplex of human RNA polymerase II (Khazak *et al.*, 1998).

Heterogeneity of RNA polymerase II preparations resulting from substoichiometric amounts of Rpb4 and Rpb7 interfered with crystallization and was circumvented by the use of a mutant strain in which the *RPB4* gene was deleted (Darst *et al.*, 1991b). Enzyme isolated from this strain lacks both Rpb4 and Rpb7 (and is therefore denoted Δ4/7) and forms large two-dimensional crystals on lipid layers, enabling structure determination at low resolution by electron crystallography (Darst *et al.*, 1991a). More recently, it has been shown that polymerase purified from cells in stationary phase has a full complement of Rpb4 and Rpb7 (Choder and Young, 1993), permitting the isolation of homogeneous, 12 subunit enzyme, which we refer to as wild-type. We report here on the crystallization and structure determination of this wild-type polymerase, and on the localization of Rpb4 and Rpb7 by direct difference analysis between the wild-type and the Δ4/7 polymerases. Finally, we discuss the functional insight provided by the location of Rpb4 and Rpb7 in light of their roles in the stress response and in the initiation of transcription.

Results

A three-dimensional reconstruction of wild-type RNA polymerase II was calculated from the computed diffraction patterns of two-dimensional crystals grown on lipid layers and imaged in the electron microscope. Data collection for the wild-type polymerase reconstruction was improved by using a wire loop to transfer crystals to the specimen grid and by washing the grids with dilute detergent solution to remove excess lipid (Asturias and Kornberg, 1995). To ensure an appropriate comparison, data for the Δ4/7 enzyme were recollected using these same procedures, and an improved reconstruction was calculated. Wild-type and Δ4/7 polymerase data sets were derived from untilted images and 64 or 69 tilted images, respectively, recorded at various tilt angles of up to 59° to the incident electron beam. Crystals formed in plane

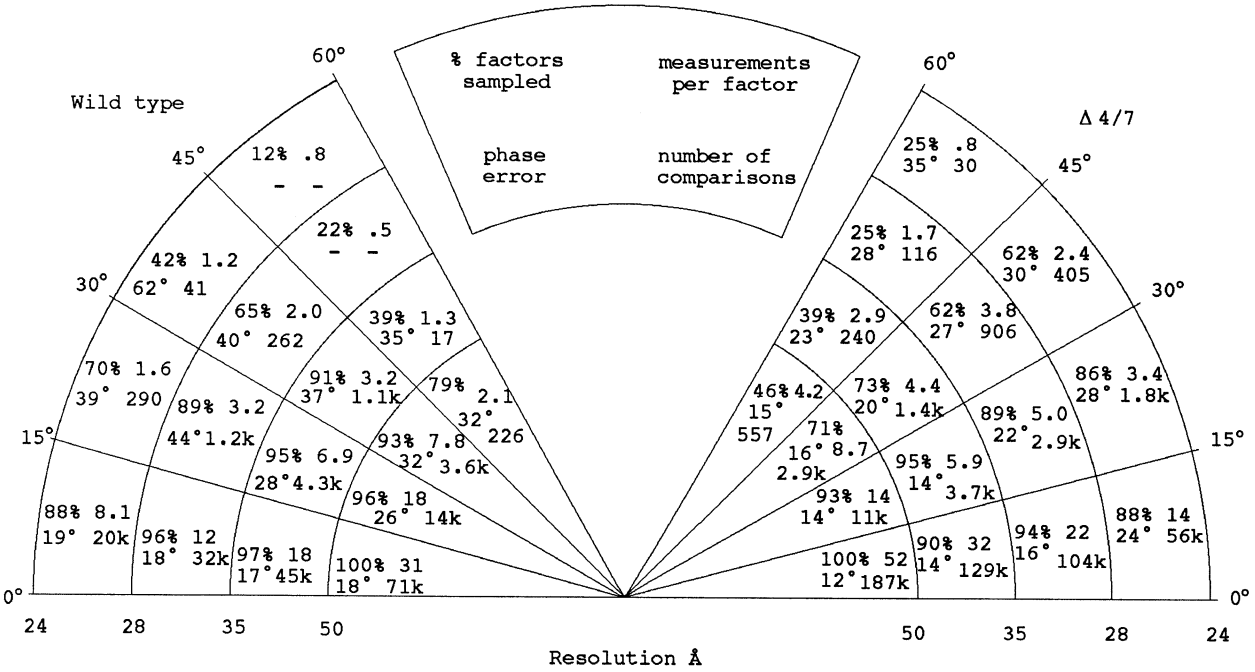

Fig. 1. Reciprocal space coverage in the wild-type and Δ4/7 reconstructions. For both the wild-type and Δ4/7 reconstructions (left and right sides of the figure, respectively), four statistics are presented in each of 16 regions of reciprocal space. The 16 regions are delimited by resolution and tilt-angular boundaries. In each region, the number in the upper left corner is the percentage of possible structure factors that were measured adequately enough to be sampled. Because, in this technique, measurements are dispersed non-uniformly along lattice lines, whether or not a structure factor is measured adequately to justify sampling can be somewhat subjective. Thus we report in the upper right corner a statistic that we call the redundancy of measurement, which is defined as the average number of measurements recorded that lie closer than half the sampling interval ($\pm$ 0.0016 Å^{-1} in this case) to each sampled structure factor. Note that only measurements in sampled regions of space are included. The number in the bottom left corner is the average phase error, defined as the average phase difference between measurements within 1/(4*T*) in *z**, where *T* is an estimate of the thickness of the molecule in the direction perpendicular to the plane of the crystal, and *z** is that direction in reciprocal space (here, *T* = 100 Å). Again, only measurements in sampled regions of space are included. The number in the bottom right corner is the number of phase comparisons used to determine the average phase error. We chose to report differences between actual phase measurements rather than differences between measurements and a curve-fit lattice line because in regions of space with few measurements, the lattice lines are relatively free to match the measurements closely.

group c2, and both data sets allowed sampling of >50% of all possible reflections to 24 Å resolution, with a missing cone of 45°. The average phase errors of individual measurements along lattice lines within 0.0025 in *z** (the direction perpendicular to the crystal plane) were 19° and 15° for the wild-type and the Δ4/7 structures, respectively (Figure 1).

Both the wild-type and the new Δ4/7 polymerase structures (Figure 2) were remarkably similar to that of the Δ4/7 polymerase reported previously (Darst *et al.*, 1991a). For the purpose of discussion, the surface shown by the right member of the pair of molecules is referred to as the 'front' side, and the surface of the left member is termed the 'back' side. Among many features common to the two structures, the 25 Å cleft (labeled 'C' in Figure 2A), which passes from the front to the back side, contains nucleic acid in a halted elongation complex (C.L.Poglitsch, G.Meredith, A.Gnatt, G.J.Jensen, W.-h.Chang and R.D. Kornberg,, in preparation) and is believed, by analogy to single subunit polymerases, to harbor the active center and bind DNA. Another feature seen in both forms of polymerase, but not discussed previously, was a groove on the front face that extended from the DNA-binding cleft towards the upper left corner (molecule on the right in Figure 2A). In the Δ4/7 polymerase, this groove appeared enclosed at some points, forming a perforated tunnel. The groove was appropriate in size for binding single-stranded nucleic acid, and was met at the upper left corner of the molecule on the right in Figure 2A by the end of another groove lying on the back face, similar in size, that also originated in the nucleic acid-binding cleft, forming a nearly continuous ring around the upper region of the polymerase.

In contrast to the previously published RNA polymerase II structure, in which the arm of protein density enclosing the cleft (labeled 'A' in Figure 2A) extended downwards, the arm appeared as a discrete domain in both enzymes at the contour level used here, and was connected with the bottom half of the molecule at lower contour levels. A further difference was in the absence here of a tunnel 35 Å in length extending through the previous structure. These differences can be accounted for by improved data quality, due to the transfer and washing techniques used and to the nearly 2-fold increase in the amount of data collected.

To reveal differences between the wild-type and Δ4/7 structures, the data sets were trimmed to analogous limits, scaled, aligned and subtracted to produce a difference map (wild-type minus Δ4/7). Because negative staining reveals only a molecular envelope, difference 'density' in areas devoid of stain within the hydrophobic core of a protein or in areas filled with stain in the large intermolecular regions is unlikely to be meaningful. To display only those differences that reasonably could be attributed to

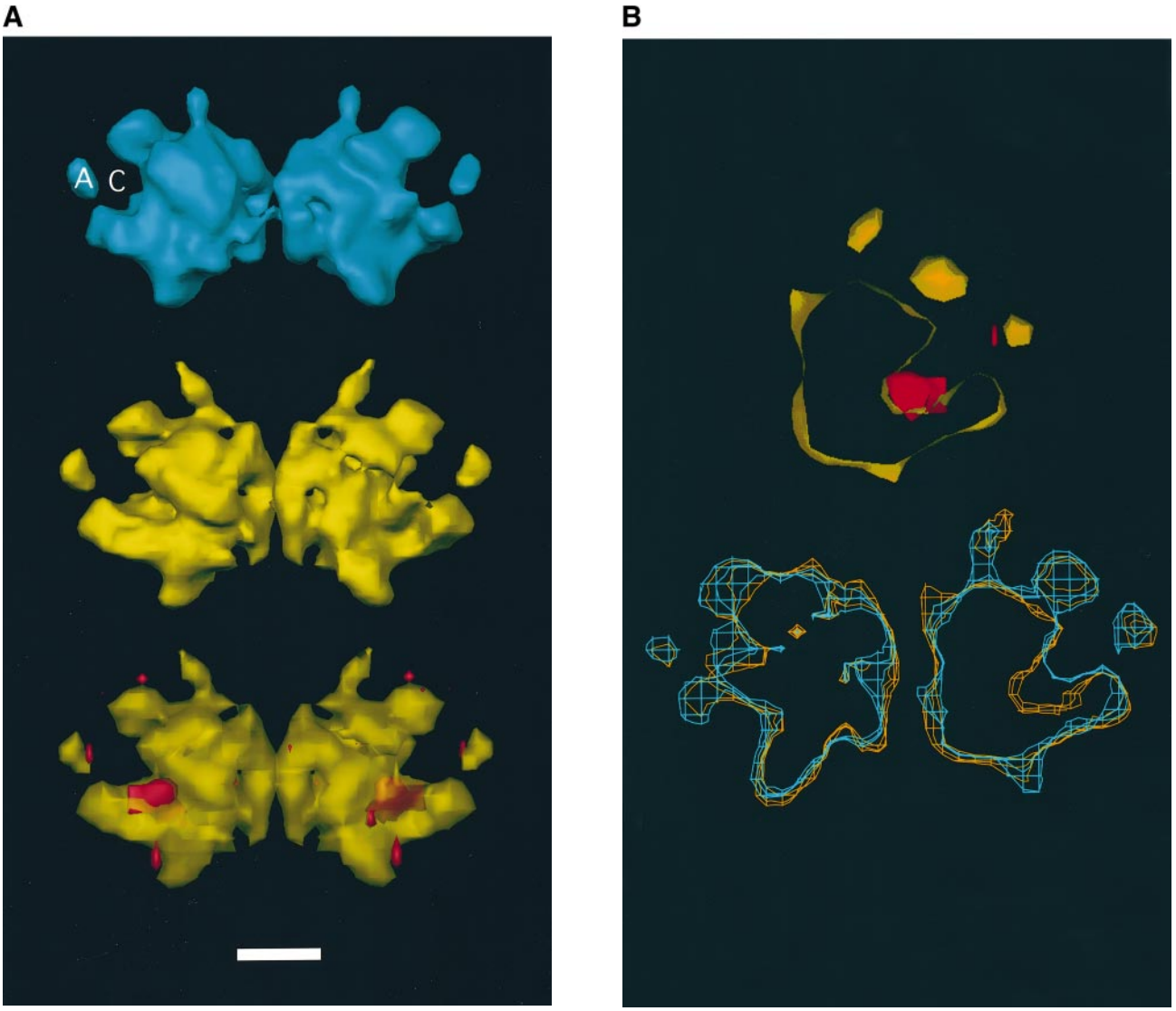

Fig. 2. (**A**) Three-dimensional reconstructions of the wild-type RNA polymerase II, the Δ4/7 RNA polymerase II and the difference between them. Both forms of RNA polymerase crystallize as dimers related by a 2-fold rotation axis in the plane of the crystal. One dimer, composed of two symmetry-averaged, identical monomers, is shown for each reconstruction. At the top, in blue, is the full reconstruction of the wild-type enzyme. Below it, in yellow, appears the full reconstruction of the Δ4/7 enzyme. The bottom display presents the wild-type–Δ4/7 differences within the boundaries described (see text) in red, contoured at 2.5 standard deviations above the mean, superimposed on a transparent view of the Δ4/7 reconstruction. The transparent view allows differences to be seen which are 'buried' in cavities or are inside the Δ4/7 reconstruction's surface. Note that on the right molecule, nearly all of the large, globular difference is covered by the front surface of the Δ4/7 reconstruction, while on the left molecule (which shows the back side view), this same globular difference is directly visible. No negative differences are seen at 2.5 standard deviations below the mean. Because negative stain is thought to partially penetrate a protein's hydrophilic shell, each polymerase is contoured at the level that encloses 70% of the expected volume. 'C' marks the 25 Å cleft that is occupied by nucleic acid in elongation complexes and is thought to harbor the active center, while 'A' marks the mobile protein arm enclosing the cleft. The scale bar represents 50 Å. (**B**) Position of Rpb4 and Rpb7 with respect to the DNA-binding cleft. The top half of the figure is a slab section from the single Δ4/7 RNA polymerase II monomer on the bottom right of (A), cut at the level of the cavity filled by Rpb4 and Rpb7, with differences at 2.5 standard deviations above the mean shown in red. The bottom half of the figure was generated by superimposing slab sections of the wild-type (blue) and Δ4/7 (yellow) dimers. The slab extends from 14 Å away from the crystal's midplane to 31 Å away. Because the slab is not centered on the midplane, the right and left halves are not mirror images, having cut through the right and left monomers of (A) at different levels, and represent independent slab sections of the same structure. The right section is a slab through the back end of the DNA-binding cleft where Rpb4 and Rpb7 are located, while the left section is a slab through the front end of the DNA-binding cleft, which does not include Rpb4 and Rpb7. Both wild-type and Δ4/7 reconstructions are contoured here at a level that encloses 100% of their expected volume to demonstrate that the cavity in the Δ4/7 enzyme corresponding to the location of Rpb4 and Rpb7 in the wild-type enzyme is not generated artifactually by contouring at inappropriately high levels. In contrast to (A), the wild-type and Δ4/7 reconstructions in (B) have been trimmed, scaled and aligned for direct comparison (see Materials and methods).

protein subunits absent from the Δ4/7 polymerase and present in the wild-type enzyme, the difference map was set to zero at all points inside the contour which enclosed 50% of the expected volume of the Δ4/7 polymerase, and at all points outside the contour which enclosed 150% of the expected volume of the wild-type polymerase. When contoured at 2.5 standard deviations above and below the mean, this map showed only one major, positive difference and three minor, positive differences (red densities in Figure 2A).

The major difference was a globular density forming part of the floor of the DNA-binding cleft, filling a cavity

in the Δ4/7 structure not seen in the wild-type structure (Figure 2A and B). The difference was centered ~10 Å away from the midplane of the crystal towards the back side. In the absence of any other large difference, we identified this density with subunits Rpb4 and Rpb7, which are known to form a single, dissociable subcomplex. The volume of this globular density, as shown contoured at 2.5 standard deviations above the mean, was 31% of the expected volume of Rpb4 and Rpb7. At slightly lower contours, where the volume increased to 100% of that expected for Rpb4 and Rpb7, the difference expanded in all directions and connected with the smaller difference directly below it.

The three minor differences between wild-type and Δ4/7 structures may result from noise in the data or from slight conformational changes induced by the presence of Rpb4 and Rpb7. The small difference just inside the arm domain ('A' in Figure 2A) was matched on the outside of the domain by a more diffuse, negative difference at lower contour levels (not shown). We suspect that these paired positive and negative differences reflect a slight inward movement of the arm domain caused by the presence of Rpb4 and Rpb7. Elsewhere it has been shown that the arm domain is mobile (Asturias *et al.*, 1997), and the movement seen here may represent a shift in the average position of the domain rather than an abrupt transition between two distinct conformations.

As a measure of significance, a difference map was calculated in the two-sided plane group p1, which imposes no symmetry, so that each structure factor derives from only half as much data and each member of the pair of polymerase molecules is determined independently. While the difference map was more noisy than before, the largest difference density by volume (contoured at 2.5 standard deviations above the mean) in both polymerase molecules was in the location assigned before to Rpb4 and Rpb7, and these differences were the highest (most significant) symmetric pair (data not shown). For further tests of significance, difference maps were calculated in the two-sided plane group c2 using alternative algorithms for trimming, scaling and aligning the maps, leading in all cases to the same conclusion about the location of Rpb4 and Rpb7 (data not shown). As a final control, we performed the same difference analysis using the data from the previous Δ4/7 structure, revealing a single large difference at 2.5 standard deviations above the mean, with the same location, general shape and approximate volume as that shown here, as well as several minor differences, including a peak just inside the arm domain (data not shown).

Perhaps the best indication of the reliability of the data is the close correspondence of the wild-type and Δ4/7 structures in regions remote from the Rpb4 and Rpb7 density (bottom of Figure 2B). Dissimilarities in the outlines of the two molecules are due to Rpb4 and Rpb7 density, conformational changes caused by Rpb4 and Rpb7, or noise. Thus the degree of dissimilarity in regions away from Rpb4 and Rpb7 provides a high estimate of the noise inherent in the technique. As the bottom of Figure 2B shows two independent sections, both 17 Å thick, about one-third of the total thickness of the molecules is presented in section here. Because the method of electron crystallography prevents data collection within the 'missing cone' of reciprocal space, the resulting models are most well determined in the midplane of the crystal, and less well determined away from the midplane. Thus the section of the molecule's total thickness that is shown here, which includes the density assigned to Rpb4 and Rpb7, displays the parts of the molecular outlines that are most appropriately used as internal controls.

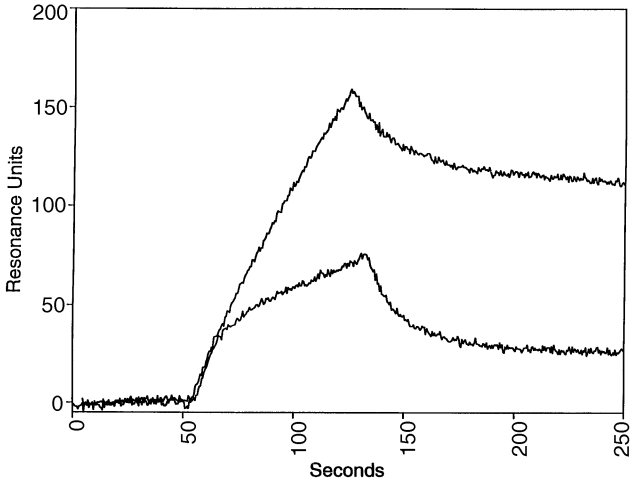

Fig. 3. Effect of Rpb4 and Rpb7 on the stability of the pre-initiation complex. A mixture of 30 μg/ml of TBP, 38 μg/ml of TFIIB, 10 μg/ml of 33 bp double-stranded DNA containing the adenovirus major late promoter sequence from –43 to –14 (5′-TTTCTGAAGG-GGGGCTATAAAAGGGGGTGGGGG-3′) and 100 μg/ml of bovine serum albumin was injected onto an 8000 resonance unit surface of wild-type polymerase (top curve) or a 8500 resonance unit surface of Δ4/7 polymerase (bottom curve). Interactions were measured with the BIAcore Biosensor (BIAcore AB). The apparent association rate was more than three times higher and the apparent dissociation rate five times lower for the wild-type than for the Δ4/7 enzyme, indicating at least a 15-fold greater affinity of the wild-type enzyme.

Elsewhere, the presence of Rpb4 and Rpb7 was shown to favor a closed conformation of the arm domain around the DNA-binding cleft and, from the requirement for these two subunits for the initiation of transcription (Edwards *et al.*, 1991), it was concluded that closure of the arm is an essential step in the initiation process (Asturias *et al.*, 1997). The difference peak seen here suggesting a tighter closure of the arm domain in the wild-type enzyme is nicely consistent, and the location of the two subunits between the two major domains that form the DNA-binding cleft suggests a mechanism whereby Rpb4 and Rpb7 contact DNA in the cleft and couple its entry to closure of the cleft.

We sought biochemical support for such a role of Rpb4 and Rpb7 by measurement of the affinities of wild-type and Δ4/7 polymerases for DNA. The measurements were made in the presence of TATA box-binding protein (TBP) and TFIIB, as occurs in the natural initiation mechanism, and which suffices for transcription in some circumstances (Parvin and Sharp, 1993). Wild-type and Δ4/7 polymerases were immobilized separately on sensor chips and tested for interaction with an adenovirus major late promoter DNA fragment–TBP–TFIIB complex by surface plasmon resonance. The apparent association rate was more than three times higher and the apparent dissociation rate five times lower for the wild-type than for the Δ4/7 enzyme (Figure 3), indicating at least a 15-fold greater affinity of

the wild-type enzyme. We conclude that Rpb4 and Rpb7 stabilize a minimal pre-initiation complex.

Discussion

The discovery that yeast RNA polymerase II with a full complement of Rpb4 and Rpb7 could be purified from cells in stationary phase enabled us to form two-dimensional crystals of wild-type polymerase suitable for structural analysis to 24 Å resolution. As the crystals were isomorphous to crystals formed with Δ4/7 enzyme, direct difference analysis was performed, locating Rpb4 and Rpb7 in the floor of the DNA-binding cleft, between the two major domains that form the cleft. A combination of small positive and negative differences suggested that Rpb4 and Rpb7 induce tighter closure of the arm domain surrounding the cleft. The finding here and elsewhere (Asturias *et al.*, 1997) that Rpb4 and Rpb7 favor closure of the arm domain around the DNA-binding cleft is easily understood in light of the position of Rpb4 and Rpb7 between the two major domains that are brought together to form the cleft (Figure 2B).

The stabilization of polymerase–DNA complexes by Rpb4 and Rpb7 can explain why these subunits are important for the stress response and for the initiation of transcription. While deletion of Rpb7 is lethal (McKune *et al.*, 1993), deletion of Rpb4 produces strains that grow slowly and are sensitive to heat, cold and starvation (Woychik and Young, 1989; Choder and Young, 1993). Because the stress response depends on the presence of transcriptionally engaged polymerase molecules paused downstream of heat shock promoters (Rasmussen and Lis, 1995), Rpb4 and Rpb7 may facilitate the stress response by stabilizing paused polymerases.

Similar reasoning can explain the role of Rpb4 and Rpb7 in the initiation of transcription. While Δ4/7 RNA polymerase II is indistinguishable from wild-type polymerase in promoter-independent initiation and elongation, it is inactive in promoter-directed initiation. The activity of Δ4/7 polymerase in promoter-directed initiation can be restored by addition of purified Rpb4 and Rpb7 or of activator proteins (Edwards *et al.*, 1991). We suggest that Rpb4 and Rpb7 sense entry of DNA into the cleft and then induce and maintain cleft closure, extending the lifetime of pre-initiation complexes and allowing other factors to interact and perform their roles. TFIIE may be a good example, as it has been located bound to the arm around the cleft in the closed conformation (Leuther *et al.*, 1996). Activators may obviate the need for Rpb4 and Rpb7 in the initiation of transcription *in vitro* by either promoting the formation of a larger number of relatively less stable initiation complexes or by stabilizing the initiation complex as do Rpb4 and Rpb7.

Materials and methods

Polymerase purification and crystallization

Wild-type and Δ4/7 polymerases were purified (Edwards *et al.*, 1990) and crystallized (Meredith *et al.*, 1996) as described, with the use of *S.cerevisiae* strains CB010 and CB010 ΔRpb4, respectively. Wild-type enzyme was derived from cells harvested during early stationary phase. Polymerase composition was verified by SDS–polyacrylamide gel electrophoresis followed by Coomassie staining and laser densitometry.

Crystal imaging and processing

Crystals were transferred to microscope grids, stained with uranyl acetate and imaged with a Philips CM12 electron microscope operating at 100 kV with a LaB6 filament at 35 000× magnification using low-dose techniques. Usually, three pictures were taken of each crystal, including one untilted image. Suitable micrographs were selected by optical diffractometry and scanned with either a Perkin-Elmer flatbed scanner or a Leaf Scanner with a 20 μm step size. Images were processed in the two-sided plane group p1 or c2 (a = 404 Å, b = 230 Å, and $\gamma = 90°$ in both cases) as described (Darst *et al.*, 1991a) by standard methods (Amos *et al.*, 1982; Henderson *et al.*, 1986). To estimate the resolution of each image, the radius at which only half of the possible structure factors were measured with signal-to-noise ratio >2 was determined, and measurements more than a few Ångstroms beyond this resolution were discarded as unreliable. During the alignment and lattice line sampling, only measurements with signal-to-noise ratios >1.4 (IQ <6 according to Henderson *et al.*, 1986) were used. Because the two monomers in the p1 asymmetric unit were nearly identical, and because the average phase error decreased from 20.1° to 19.2° upon c2 averaging for the wild-type reconstruction, the figures were produced using symmetry-averaged, c2 data. Smooth curves were fit to the reciprocal space lattice lines and were sampled at spacings corresponding to a unit cell 300 Å thick to obtain three-dimensional Fourier terms. In regions where there were no measurements within about half the sampling interval along a lattice line or where the measurements were in poor agreement, no structure factors were sampled. Reconstructions were visualized with the XtalView software package (McCree, 1992), and surface envelopes were generated by Synu (Hessler *et al.*, 1992). Predicted protein volumes were calculated using the estimate 1.21 $Å^3$/Da.

Image processing was facilitated by three new FORTRAN programs by G.Jensen, which are available upon request. The first finds initial lattice vectors from an image transform for subsequent refinement, and the second finds vertices for cutting out continuous regions of crystal using the results of the 'unbending' process outlined in Henderson *et al.* (1986). The third program collects the statistics shown in Figure 1.

Difference analysis

Wild-type and Δ4/7 polymerase crystals were isomorphous, allowing direct difference calculation after appropriate trimming, scaling and aligning. Each set of structure factors contained >50% of the expected reflections to 24 Å resolution, with a missing cone of 45°. All structure factors outside these limits were discarded. Amplitude scaling was done in four separate bins (250–50 Å, 50–35 Å, 35–28 Å and 28–24 Å) to diminish any resolution-dependent differences in contrast transfer by multiplying all the wild-type structure factor amplitudes within a given bin by the appropriate scale factor to equalize the mean amplitudes of the wild-type and the Δ4/7 sets of structure factors. Reconstructions were aligned along the a and c axes of the unit cell by defining the crystallographic 2-fold symmetry axis as the b axis, while alignment along b was accomplished by minimizing weighted phase differences between the sets of structure factors. Differences were calculated directly in real space or equivalently in reciprocal space by vector subtraction.

Surface plasmon resonance measurements

All proteins were diluted in running buffer (40 mM HEPES pH 7.6, 7.5 mM $MgCl_2$, 120 mM potassium acetate, 0.005% Surfactant P-20) from concentrated stock solutions prior to use. Wild-type and Δ4/7 polymerases were immobilized in 100 mM sodium acetate pH 5.0 at 100 μg/ml on CM5 research-grade sensor chips with the use of an amine-coupling kit (BIAcore AB). Blank surfaces were prepared by introduction of buffer without protein. Non-covalently bound proteins were removed by washing with running buffer containing 1 M potassium acetate. Mixtures of TBP, TFIIB, double-stranded DNA containing adenovirus major late promoter sequence, and bovine serum albumin were incubated on ice for 20 min and then injected onto a polymerase surface at room temperature in running buffer at a flow rate of 15 μl/min. Interactions were measured with the BIAcore Biosensor (BIAcore AB). TBP and TFIIB were purified according to Myers *et al.* (1997).

Acknowledgements

We thank Steve Orlicky and Al Edwards for providing purified recombinant Rpb4 and Rpb7 complex, and Seth Darst for helpful advice. G.J.J. was supported by a Medical Scientist Training Program grant (GM07365) provided by the National Institute of General Medical Sciences at the NIH. This research was funded by NIH grant AI21144 to R.D.K.

References

Amos,L.A., Henderson,R. and Unwin,P.N. (1982) Three-dimensional structure determination by electron microscopy of two-dimensional crystals. *Prog. Biophys. Mol. Biol.*, **39**, 183–231.

Asturias,F.J. and Kornberg,R.D. (1995) A novel method for transfer of two-dimensional crystals from the air/water interface to specimen grids. *J. Struct. Biol.*, **114**, 60–66.

Asturias,F.J., Meredith,G.D., Poglitsch,C.L. and Kornberg,R.D. (1997) Two conformations of RNA polymerase II revealed by electron crystallography. *J. Mol. Biol.*, **272**, 536–540.

Choder,M. and Young,R.A. (1993) A portion of RNA polymerase II molecules has a component essential for stress response and stress survival. *Mol. Cell. Biol.*, **13**, 6984–6991.

Darst,S.A., Kubalek,E.W. and Kornberg,R.D. (1989) Three-dimensional structure of *Escherichia coli* RNA polymerase holoenzyme determined by electron crystallography. *Nature*, **340**, 730–732.

Darst,S.A., Edwards,A.M., Kubalek,E.W. and Kornberg,R.D. (1991a) Three-dimensional structure of yeast RNA polymerase II at 16 Å resolution. *Cell*, **66**, 121–128.

Darst,S.A., Kubalek,E.W., Edwards,A.M. and Kornberg,R.D. (1991b) Two-dimensional and epitaxial crystallization of a mutant form of yeast RNA polymerase II. *J. Mol. Biol.*, **221**, 347–357.

Dezelee,S., Wyers,F., Sentenac,A. and Fromageot,P. (1976) Two forms of RNA polymerase B in yeast. *Eur. J. Biochem.*, **65**, 543–552.

Edwards,A.M., Darst,S.A., Feaver,W.J., Thompson,N.E., Burgess,R.R. and Kornberg,R.D. (1990) Purification and lipid-layer crystallization of yeast RNA polymerase II. *Proc. Natl Acad. Sci. USA*, **87**, 2122–2126.

Edwards,A.M., Kane,C.M., Young,R.A. and Kornberg,R.D. (1991) Two dissociable subunits of yeast RNA polymerase II stimulate the initiation of transcription at a promoter *in vitro*. *J. Biol. Chem.*, **266**, 71–75.

Henderson,R., Baldwin,J.M., Downing,K.H., Lepault,J. and Zemlin,F. (1986) Structure of purple membrane from *Halobacterium halobium*: recording, measurement and evaluation of electron micrographs at 3.5 Å resolution. *Ultramicroscopy*, **19**, 147–178.

Hessler,D. *et al*. (1992) Programs for visualization in three-dimensional microscopy. *Neuroimage*, **1**, 55–67.

Khazak,V., Estojak,J., Cho,H., Majors,J., Sonoda,G., Testa,J.R. and Golemis,E.A. (1998) Analysis of the interaction of the novel RNA polymerase II (pol II) subunit hsRPB4 with its partner hsPRB7 and pol II. *Mol. Cell. Biol.*, **18**, 1935–1945.

Leuther,K.K., Bushnell,D.A. and Kornberg,R.D. (1996) Two-dimensional crystallography of TFIIB– and IIE–RNA polymerase II complexes: implications for start site selection and initiation complex formation. *Cell*, **85**, 773–779.

McCree,D.E. (1992) A visual protein crystallographic software system for XII/XView. *J. Mol. Graphics*, **10**, 44–46.

McKune,K., Richards,K.L., Edwards,A.M., Young,R.A. and Woychik,N.A. (1993) Rpb7, one of two dissociable subunits of yeast RNA polymerase II, is essential for cell viability. *Yeast*, **9**, 295–299.

Meredith,G.D., Chang,W.H., Li,Y., Bushnell,D.A., Darst,S.A. and Kornberg,R.D. (1996) The C-terminal domain revealed in the structure of RNA polymerase II. *J. Mol. Biol.*, **258**, 413–419.

Myers,L.C., Leuther,K., Bushnell,D.A., Gustafsson,C.M. and Kornberg,R.D. (1997) Yeast RNA polymerase II transcription reconstituted with purified proteins. *Methods*, **12**, 212–216.

Parvin,J.D. and Sharp,P.A. (1993) DNA topology and a minimal set of basal factors for transcription by RNA polymerase II. *Cell*, **73**, 533–540.

Polyakov,A., Severinova,E. and Darst,S.A. (1995) Three-dimensional structure of *E.coli* core RNA polymerase: promoter binding and elongation conformations of the enzyme. *Cell*, **83**, 365–373.

Rasmussen,E.B. and Lis,J.T. (1995) Short transcripts of the ternary complex provide insight into RNA polymerase II elongational pausing. *J. Mol. Biol.*, **252**, 522–535.

Ruet,A., Sentenac,A., Fromageot,P., Winsor,B. and Lacroute,F. (1980) A mutation of the B220 subunit gene affects the structural and functional properties of yeast RNA polymerase B *in vitro*. *J. Biol. Chem.*, **255**, 6450–6455.

Schultz,P., Celia,H., Riva,M., Darst,S.A., Colin,P., Kornberg,R.D., Sentenac,A. and Oudet,P. (1990) Structural study of the yeast RNA polymerase A: electron microscopy of lipid-bound molecules and two-dimensional crystals. *J. Mol. Biol.*, **216**, 353–362.

Sousa,R., Chung,Y.J., Rose,J.P. and Wang,B.C. (1993) Crystal structure of bacteriophage T7 RNA polymerase at 3.3 Å resolution. *Nature*, **364**, 593–599.

Woychik,N.A. and Young,R.A. (1989) RNA polymerase II subunit Rpb4 is essential for high- and low-temperature yeast cell growth. *Mol. Cell. Biol.*, **9**, 2854–2859.

Received September 1, 1997; revised and accepted February 6, 1998